Nonequilibrium modeling of heat and mass transfer with partial condensation in a tube-type interface for heat integrated distillation column

Kunio Kataoka, Hideo Noda, Tadahiro Mukaida, Mampei Kaneda
Kansai Chemical Engineering Co., Ltd.
and
Masaru Nakaiwa
National Institute of Advanced Industrial Science and Technology

Prepared for Presentation at 2005 AIChE Annual Meeting/   /01D01

Unpublished

INTRODUCTION

This is a fundamental study running along the governmental project line for development of energy-saving distillation technology in chemical industry in relation with the protection against global warming. If the energy discharged from the overhead condenser were utilized for the energy supplied to the reboiler, an energy-saving distillation could be realized with a very small heat source or without any outside heat source. In order to pump up the energy from the condenser to the reboiler, the rectifying section should be pressurized by a compressor to make its temperature level higher than that of the reboiler/stripping section. Figure 1 shows that an internal heat integration can be realized by contacting the higher-temperature rectifying section with the lower-temperature stripping section, where the latent heat released by partial condensation of the rectifying section vapor can be utilized to evaporate partially the stripping section liquid (internal reflux). The review paper by Nakaiwa et al. (2003) surveyed recent investigations on the heat integrated distillation column (HIDiC) technology and introduced various internal structures for heat integration. Recently, a commercial-scale pilot plant of packed-column-type HIDiC system was firstly constructed as a C5 splitter in a petrochemical company and successfully achieved the target of more than 30% energy saving (Horiuchi et al., 2005).

The present study pays attention to design of built-in interfaces for large-diameter commercial-scale plate-column-type HIDiC systems, that is, design of built-in tubes for internal heat exchange between the higher-temperature rectifying section and the lower-temperature stripping section. The heat transfer tube having a U-tube-shaped flow passage inside is protruded from the vapor zone over a stage of the rectifying section into the foam layer bubbling on a stage of the stripping section. As schematically shown in Fig.2, the vapor mixture supplied into the tube from the rectifying section flows through the inside flow passage with partial condensation of less-volatile components and the remaining vapor mixture flows out into the vapor zone on the above stage of the same rectifying section. The vapor feed rate usually depends on the pressure drop across the bubbling plate located between the inlet and outlet of the tube. The bubbling liquid on a stage of the stripping section undergoes partial vaporization of more-volatile components over the outside surface of the tube due to the latent heat of condensation released from inside the tube.

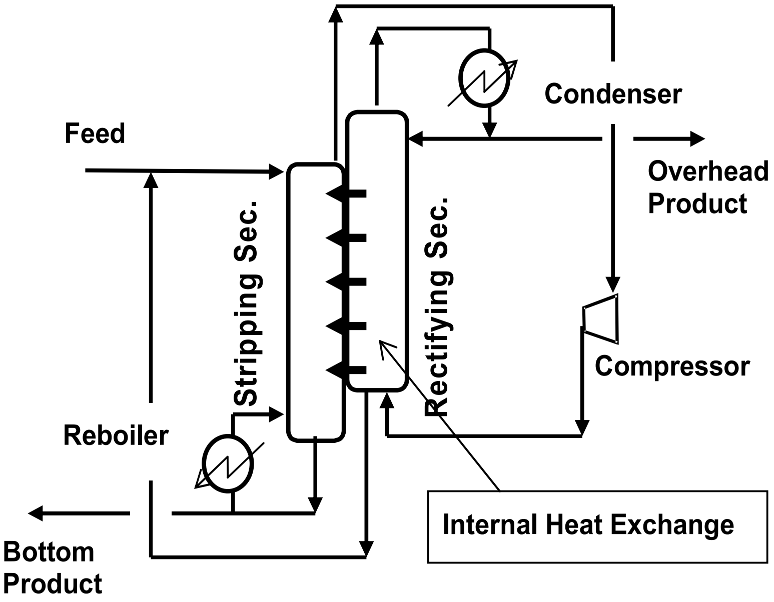

Figure 1 Schematic picture of a heat integrated distillation column (HIDiC) system.

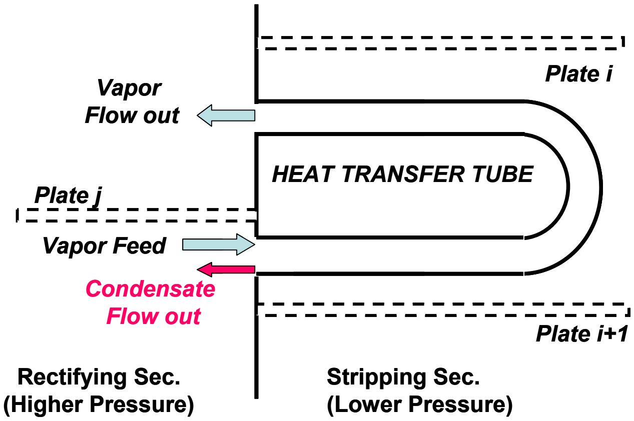

Figure 2 Heat transfer tube for large-scale plate-column-type HIDiC systems.

The purpose of the present study was to construct a thermal design model based on simultaneous heat and mass transfer accompanied with condensation inside a heat transfer tube. The model can be generalized to analyze the internal heat exchange capacity as the key technology for plate-type heat integrated distillation column (HIDiC) systems from various engineering viewpoints. The experimental observation of heat and mass transfer in a U-tube type heat transfer simulator with an isothermal equilibrium model was reported in the previous paper (Kataoka et al., 2005). Usually in the analysis of condensation heat transfer, the temperature of condensable vapor phase is assumed equal to the vapor-liquid interface temperature. At the present stage, there is no investigation of simultaneous heat and mass transfer with condensation taking into account the non-isothermal condition between the vapor phase and the interface of condensation from a view point of non-equilibrium thermodynamics.

MODEL SPECIFICATION AND ASSUMPTION

As shown in Fig.3, only for simplification of modeling, a straight heat transfer tube can be assumed instead of the practical U-shaped tube. The model deals with a saturated benzene-toluene vapor mixture supplied at a feed rate F mol/s, temperature T_F ℃ and pressure P atm into a circular tube of length $z_T = 1$ m and inside diameter $D = 0.04$ m. The pressure drop over the tube length (of the order of 0.5 kPa) can be assumed negligibly small compared to the total pressure (＞0.1MPa) when the variables, coefficients and parameters related with heat and mass transfer are estimated. The tube wall temperature is also assumed to be kept at T_S ℃ by the surrounding bubbling liquid.

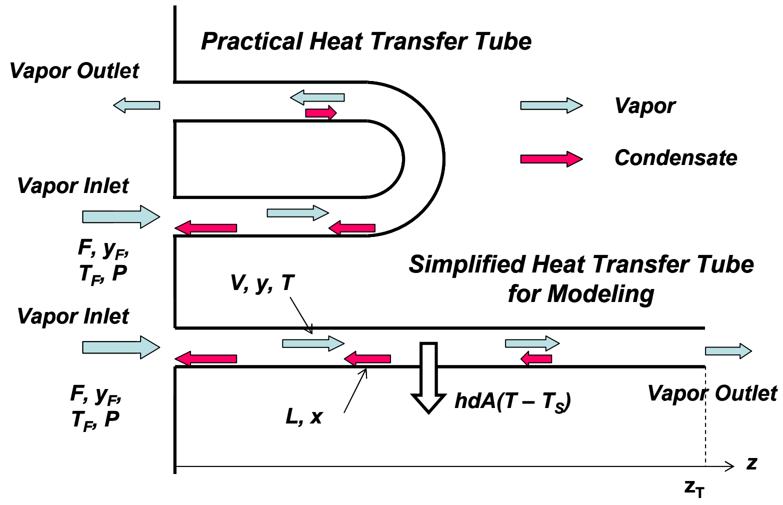

Figure 3 Configuration of heat transfer tube simplified for modeling

The following two assumptions provide a basic key concept of this study:

(1) heat transfer coefficient h W/m^{2}K is proportional to local mass flux of the partial condensation

(2) vapor phase temperature is kept constant over the flow cross-section but not equal to the condensate liquid interface temperature owing to a temperature jump due to a large release of latent heat (Non-equilibrium model)

For an isothermal equilibrium model, the liquid interface is assumed to be at the same temperature as the vapor phase. For the case of benzene-toluene system, a mass flux due to condensation of two condensable vapors directly generates a large release of latent heat on the liquid surface (heat source), which should be absorbed through the condensate film (heat sink) into the tube wall. This suggests that a large coupling effect should result from the large enthalpy change of the phase transition at the interface with a temperature jump (Kjelstrup and Bedeaux, 2005). The heat flux is largely influenced by the mass flux, vice versa. The latter assumption suggests it necessary to consider a non-equilibrium model. It is very difficult how to express the assumption of local non-equilibrium based on non-equilibrium thermodynamics for the practical model. The temperature jump can be taken into account modifying the phase equilibrium coefficient.

$$y_i = B_i K_i x_i \tag{1}$$

where $B_1 \geq 1$ for more-volatile component (benzene) and $B_2 \leq 1$ for the less-volatile component (toluene). The phase equilibrium coefficient K_i in the isothermal condition is estimated by giving local vapor temperature and total pressure to the Antoine empirical relation. The isothermal equilibrium model ($B_i = 1$) assumes the vapor and condensate to be at an equal temperature on the interface. The non-equilibrium model is based on an assumption of some temperature jump on the liquid surface.

The simulation analysis was made with various combinations of operation pressure, vapor supply conditions (feed rate, feed temperature and composition depending on pressure), and tube wall temperature to determine local variation of the following variables inside the tube: (1) temperature and concentration of each component in vapor and liquid film streams; (2) mass-flux of partial condensation, (3) heat-flux, (4) vapor and liquid flow rates and (5) heat transfer coefficient.

GOVERNING EQUATION OF HEAT AND MASS TRANSFER

It should be considered that the countercurrent stream of the condensate has a temperature difference $T - T_s$ across the condensate film when the liquid film temperature is estimated. A shell balance for heat and mass transfer is set up over a differential control volume shown in Fig.4. When the concentration $x_i{**}$ of the on-site condensate is estimated, there is no temperature jump: $T{**} - T = 0$ for the isothermal equilibrium model

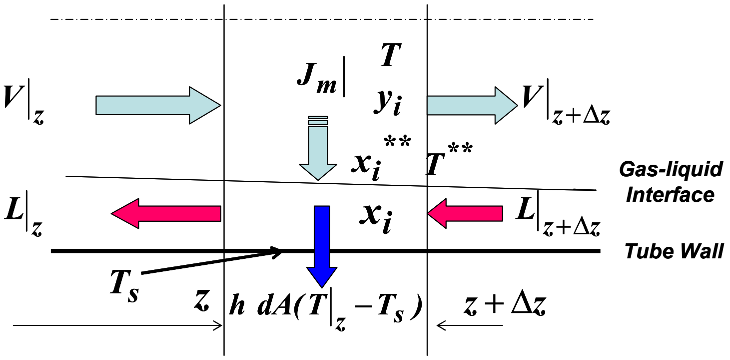

Figure 4 Non-equilibrium countercurrent model setting up a heat and mass balance over a differential control volume..

whereas there is some temperature jump: $T^{**} - T$ for the non-equilibrium model.

A set of fundamental equations about heat and mass balance at steady state are given as

(Local mass balance) $DL - DV = 0$ and $D(Lx_i) - D(Vy_i) = 0$ (2)

(Local enthalpy balance) $D(LH_L) - D(VH_V) - h\ dA(T - T_s) = 0$ (3)

where the liquid enthalpy is estimated at a local condensate film temperature averaged $(T + T_s)/2$ assuming a linear temperature profile

(Local mass balance of condensation) $D(Vy_i) - D(Lx_i^{**}) = 0$ (4)

This equation indicates that the local composition x_i^{**} of condensate should be estimated taking into account some temperature jump $T^{**} - T$ for the non-equilibrium model.

Equation 1 introduces the effect of non-equilibrium in terms of the degree of deviation from equilibrium: B_i :

(Non-isothermal phase relation) $y_i = B_i K_i x_i^{**}$□□(

This modification coefficient B_i implies that the liquid surface is at a temperature slightly higher than the vapor phase. For example, the degree of non-equilibrium was defined as B=95% when $B_2 = 0.95$.

$$\Sigma y_i = 1 \qquad \Sigma x_i = 1 \qquad \Sigma x_i^{**} = 1 \qquad \text{and} \qquad D = \frac{d}{dz}$$

(Boundary conditions) at $z = 0$; $V = F$; $Vy_i = Fy_{F,i}$; $T = T_F$ (5)

at $z = z_T$; $L = 0$ (6)

The heat transfer coefficient can be assumed to consist of forced convection and condensation in parallel as follows:

(Heat transfer coefficient) $h = h_c + J_m \lambda_m /(T - T_w)$ (7)

where the forced convection contribution is assumed to be $h_c = 300$ W/m^{2}K and the second term can be expressed to be local mass-flux J_m of condensation multiplied by latent heat of local condensate mixture.

This model consisting of four differential equations Eqs.1 to 4 can be calculated numerically by Newton-Raphson method. As shown in Fig.3, only for simplification of modeling, the heat transfer tube has one-way single passage, one end of which serves as the outlet of the residual vapor and the other end serves as the inlet of the fresh vapor supplied from the rectifying section as well as the outlet of condensate stream.
The heat transfer specifications for calculation are given by Table 1.

Table 1 Conditions and variables listed for simulation analysis

Variable	
Total pressure inside heat transfer tube (atm)	Constant specified:1.5~2.0
Feed rate of vapor mixture (mol/s)	variable
Feed temperature in centigrade	variable
Feed composition (benzene in mole fraction) (Feed vapor is assumed to be saturated.)	Depending on temperature and pressure of feed
Tube wall temperature in centigrade	Constant specified
Temperature difference between feed and tube wall (Inlet condition)	Constant specified
Heat Transfer Test Tube	
Length (m)	1.0
Inside diameter (mm)	40
Heat transfer area (m^2)	0.126

RESULTS AND DISCUSSION

The numerical analysis was made to solve the model equations for a benzene-toluene binary mixture. The conditions specified for simulation analysis is restricted taking into account the situation of HIDiC systems. As the stripping section is assumed to be operated at normal pressure, the vapor feed pressure corresponds to the compression ratio for the HIDiC systems. Generally speaking, the feed composition of the saturated vapor supplied from the rectifying section should be more-volatile component (benzene) rich. This condition restricts the upper limit of feed temperature depending on the compression ratio. The wall temperature of the heat transfer tube should be specified from the less-volatile component (toluene) rich condition of the stripping section. If the vapor feed pressure (compression ratio) is varied, the feed vapor composition automatically varies. The majority of the simulation analysis was made with the isothermal equilibrium model assuming that the on-site condensate on the interface should have the same temperature as the vapor phase. The non-equilibrium model was treated in terms of an assumed degree of deviation from phase equilibrium in place of a temperature jump.

(1) Effect of Vapor Feed Temperature

The simulation was made varying the vapor feed temperature at a constant pressure without deviation from equilibrium: B=100%. For comparison, the feed rate was also fixed (see the table shown below). The higher temperature condition (condition A) giving the higher concentration of less-volatile component indicates the vapor supplied from the lower stage position of the rectifying section.

Table 2 Simulation condition analyzing the effect of vapor feed temperature

Condition A	P=1.5 atm, F=0.01 mol/s, B=100%	T_F=115C, T_S=105C, $y_{F,1}$=0.433
Condition B	P=1.5 atm, F=0.01 mol/s, B=100%	T_F=110C, T_S=95C, $y_{F,1}$=0.600

Figure 5 shows two diagrams of composition trajectory along the heat transfer tube. It should be kept in mind that the condensate flows from right to left while the vapor flows from left to right. Therefore the vapor is almost in equilibrium with the on-site condensate stream near the vapor exit, that is, the initiation point of condensate stream. On the other hand, the condensate stream discharged through the vapor inlet from the tube is far from equilibrium with the vapor fed there owing to the accumulation effect of the countercurrent system.

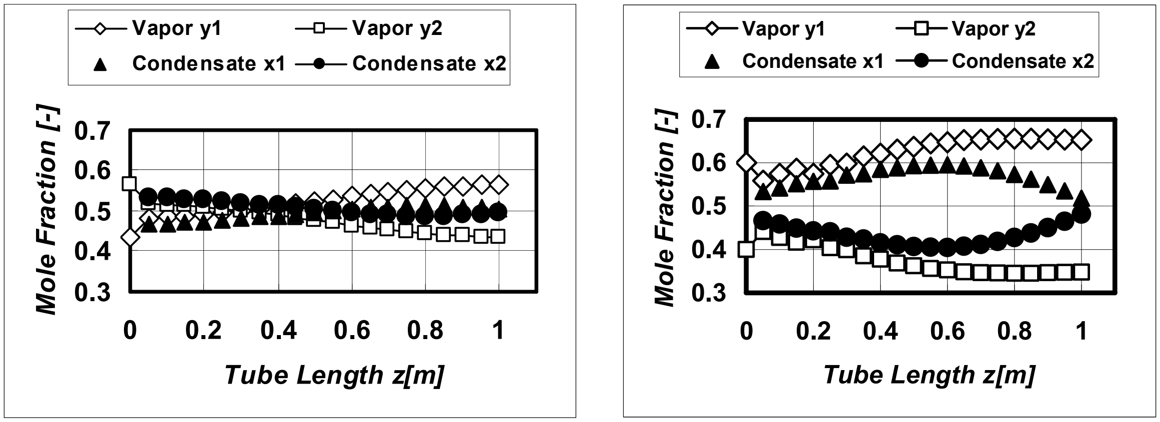

Figure 5 Comparison of composition trajectory along tube length.
(mole fraction of benzene and toluene y1, y2 in vapor, x1, x2 in condensate liquid)
(Left diagram) Condition A. (Right diagram) Condition B.

The left diagram shows less change in concentration than the right diagram.
This depends on how much the feed contains less-volatile component.
As shown in Fig.6, condition A gives larger fraction of condensation in the total heat flux, that is, larger coefficients of heat transfer than condition B.

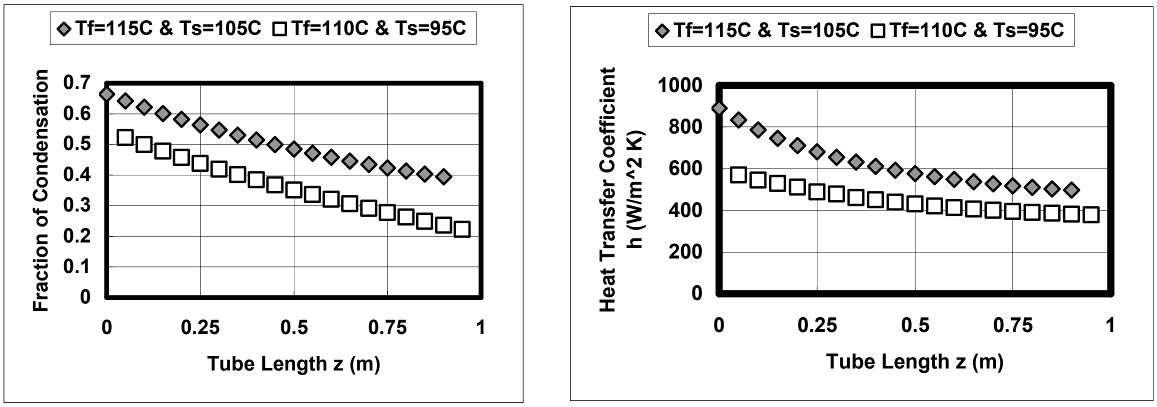

Figure 6 Local fraction of condensation in total heat transfer and local coefficient of heat transfer compared between condition A and B.

It should be noticed that the condensation heat transfer is not predominant (less than 50%) over the almost whole passage of the tube in condition B. The condition, which cannot obtain a sufficient increase in the internal reflux liquid of the rectifying section, is not appropriate for HIDiC systems. These results may suggest that there is a lower limit of feed temperature depending on vapor feed pressure

(2) Effect of Vapor Feed Rate

The simulation varying the vapor feed rate only is easy because the remaining conditions can easily be fixed. The feed vapor pressure $\boldsymbol{P = 2.0}$ atm implies the compression ratio=2, that is, to compress the vapor from the top of the stripping section operated at normal pressure into the rectifying section operated at 2 atm.

Table 3 Simulation condition analyzing the effect of vapor feed rate.

Condition C	F=0.01 mol/s	P=2.0 atm, T_F=125C, T_S=100C, $y_{F,1}$=0.469, B=100%
Condition D	F=0.035 mol/s	P=2.0 atm, T_F=125C, T_S=100C, $y_{F,1}$=0.469, B=100%

The simulation results, obtained without deviation from equilibrium: B=100%, are shown in Figs. 7 and 8. As distinct from condition C, the composition trajectory for condition D shown in the right diagram of Fig.7 does not show any discernibly large change in concentration. This is due to the fact that the vapor feed sufficient for condensation was supplied. This implies that if the feed rate is raised, most of great change in vapor and liquid concentrations will occur in the inlet region near the vapor inlet owing to the large condensation heat transfer.

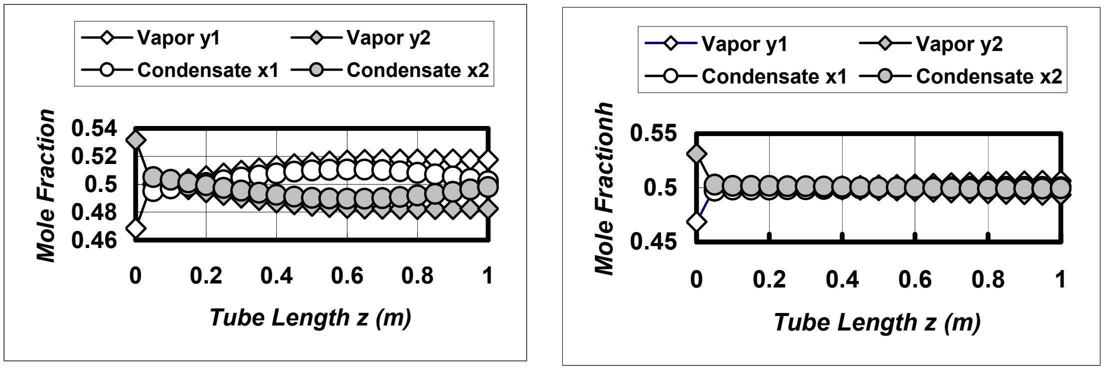

Figure 7 Comparison of composition trajectory between condition C and D.

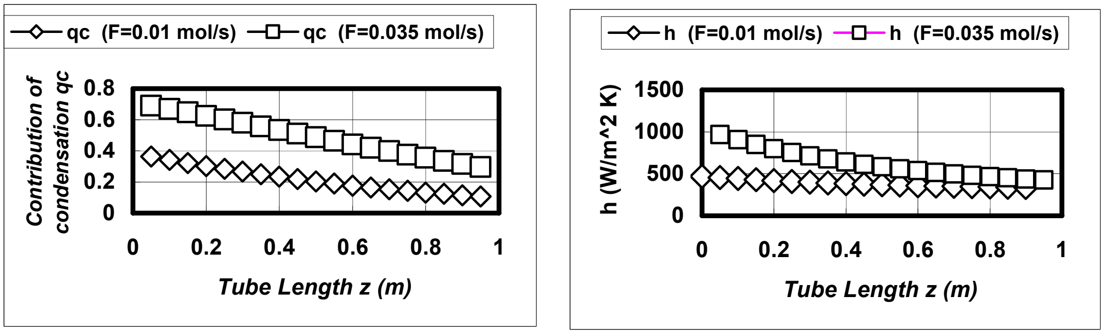

Figure 8 Local fraction of condensation in total heat transfer and local coefficient of heat transfer compared between condition C and D.

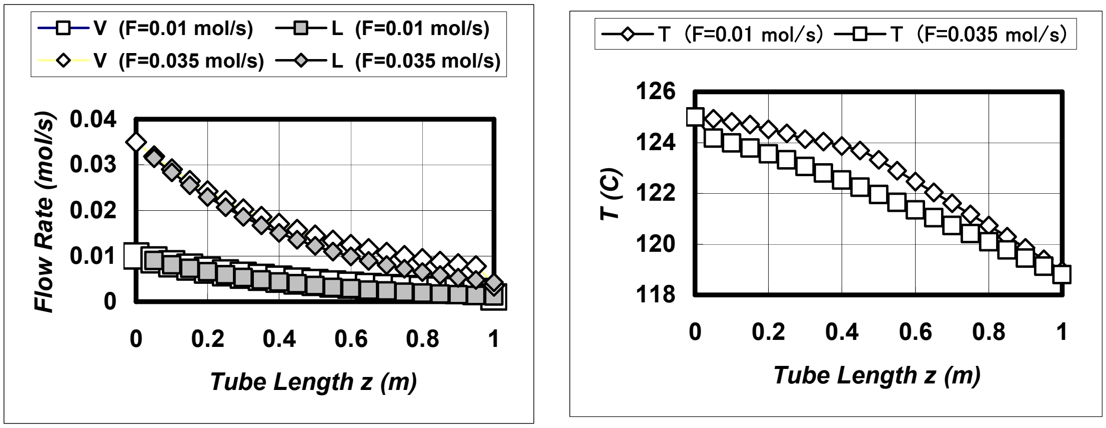

Figure 9 Variation of vapor and liquid flow rates and vapor temperature compared between condition C and D.

It can be considered that the larger the vapor feed rate, the larger the heat transfer rate. As shown in Fig.8, the heat transfer rate is controlled mostly by condensation when the feed rate is large. It can be seen from Fig.9 (Right diagram) that the vapor temperature is going down faster for condition D than for condition C. The vapor temperature going down along the tube is due to the cooling effect of convective heat transfer as well as the decreasing mole fraction of less-volatile component.

(3) Effect of Vapor Feed Pressure

The effect of vapor feed pressure was also considered for the following two conditions. The simulation results are shown in Figs. 10 and 11..

Table 4 Simulation condition analyzing the effect of vapor feed pressure.

Condition E	P=1.8 atm	T_F=120C, T_S=105C, F=0.01 mol/s, $y_{F,1}$=0.498, B=100%
Condition F	P=1.5 atm	T_F=115C, T_S=100C, F=0.01 mol/s, $y_{F,1}$=0.433, B=100%

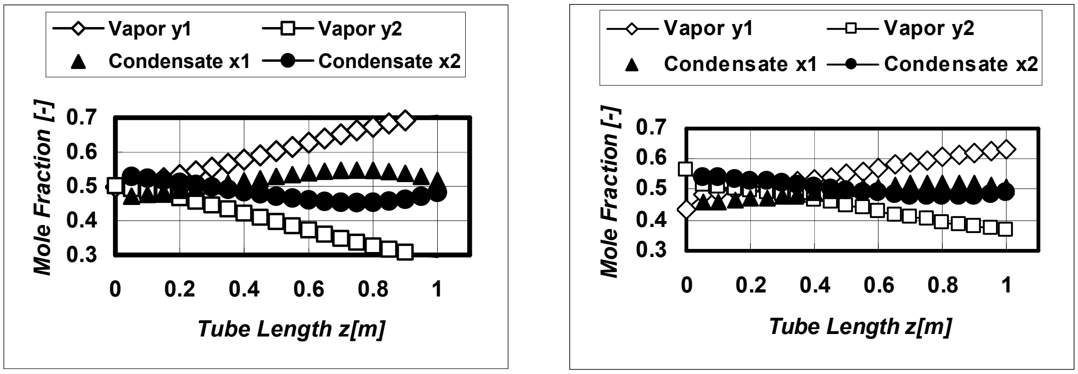

Figure 10 Composition trajectory. (Left diagram) condition E, (Right diagram) condition F.

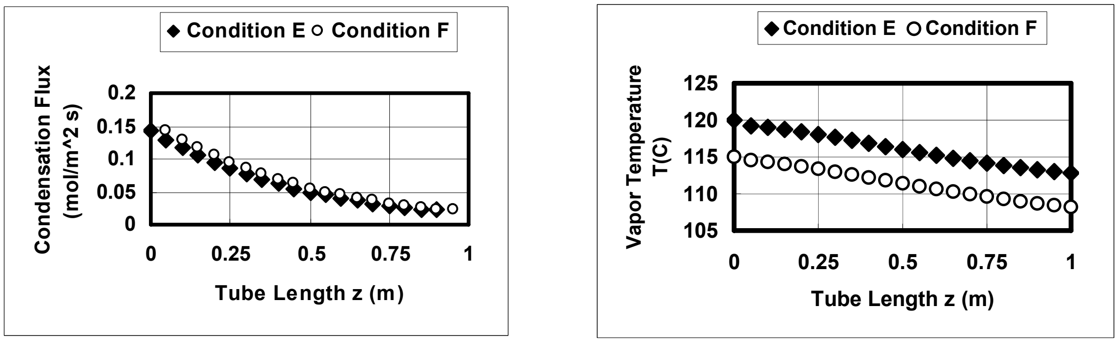

Figure 11 Condensation mass-flux and vapor temperature compared between condition E and F.

There is no discernible difference in the variation of condensation mass-flux and vapor temperature except for a small difference in the composition trajectory between condition E and F. The vapor feed contains more less-volatile component for condition F than condition E but there is no discernible difference in condensation mass-flux between the two conditions because of the equal feed rate.

(4) Heat Transfer Characteristics: Internal Heat Exchange

It is of great importance to consider what the key variable controlling the internal heat exchange is for the case of heat transfer tubes because the vapor flows decreasing the flow rate accompanied with change in composition and temperature through tubes.
For the purpose of HIDiC systems, the internal reflux should be increased by the partial condensation of less-volatile components in the rectifying section.
Table 5 indicates conditions summarized for all the simulation analysis using the isothermal equilibrium model, where the feed rate can be varied freely.

Table 5 Simulation analysis conditions for isothermal equilibrium model

No.	P (atm)	T_F (℃)	T_S (℃)	No.	P (atm)	T_F (℃)	T_S (℃)
#1	1.5	110	95	#7	1.8	120	100
#2	1.5	110	100	#8	1.8	120	105
#3	1.5	112.5	100	#9	1.8	122.5	100
#4	1.5	115	90	#10	1.8	125	100
#5	1.5	115	100	#11	2.0	125	100
#6	1.5	115	105				

Figure 12 shows the results of simulation summarized with respect to the total heat transfer rate attained by a tube. It has been found that the heat transfer rate is almost linearly proportional to the vapor feed rate irrespective of the feed temperature and pressure (compression ratio). This can be attributed to the fact that the latent heat of vapor mixture does not vary so much with temperature and pressure and the release of latent heat is exactly proportional to the condensation flux, i.e. vapor feed rate. It can be considered that some scatter of calculation results is attributable to the difference in the concentration of the vapor feed.

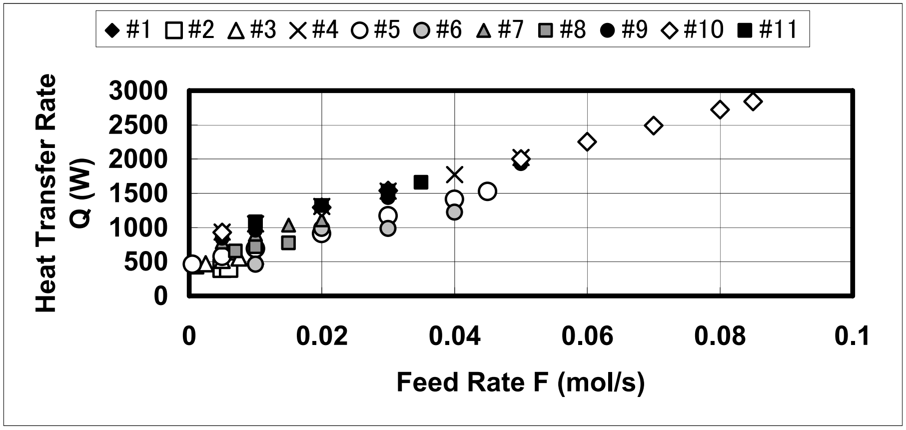

Figure 12 Heat transfer rates calculated for various conditions listed in Table 5.

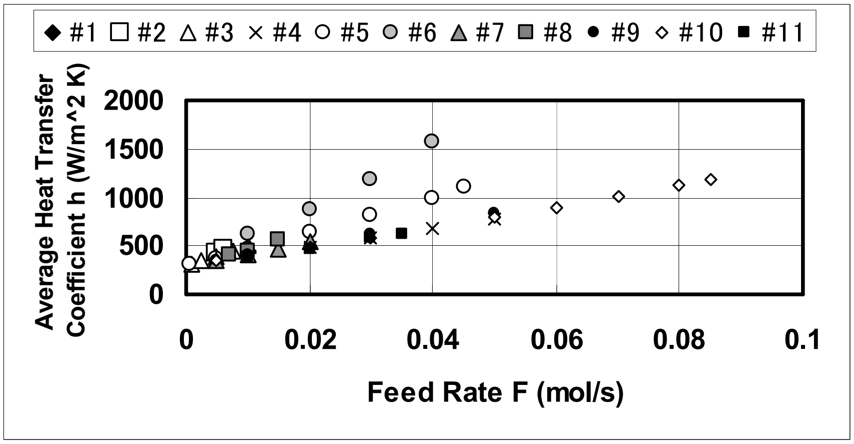

Figure 13 Heat transfer coefficients averaged over the whole tube length calculated for various conditions listed in Table 5..

The heat transfer coefficient was assumed to be almost proportional to the condensate mass-flux, although a small effect of convection was taken into account. It has been found from Fig.13 that the averaged heat transfer coefficients divide into several groups depending on the initial temperature difference, i.e. $T_F - T_s$.

This can be understood from the fact (e.g. Kreith, 1976) that the average value of conductance for a vapor condensing on a plate is usually expressed as

$$\overline{h_c} = 0.943\left[\frac{\rho_L(\rho_L - \rho_V)gh'_{fg}\kappa^3}{\mu_L L(T_{SV} - T_S)}\right]^{1/4}$$

where h'_{fg} is the enthalpy change of the vapor in condensing to liquid and subcooling to the average temperature of the condensate film.

(5) Effect of Non-equilibrium

It can be conjectured from a viewpoint of non-equilibrium thermodynamics theory (Kjelstrup and Bedeaux, 2005) that a large mass-flux of condensation may form some degree of temperature jump on the liquid-surface, as shown in Fig.14. Even at steady state, a release of large enthalpy of phase transition on the liquid surface (heat source) should be absorbed from the heat sinks on both sides, that is, the liquid film side as well as the vapor phase side. The previous model should have taken into account directly the coupling effect between the heat and mass fluxes. The equilibrium relation can be modified by estimating the on-site condensate composition at a temperature a little bit higher than that of the vapor phase. Similar simulation analysis was made taking into account the deviation from isothermal equilibrium with the assumed modification coefficient.

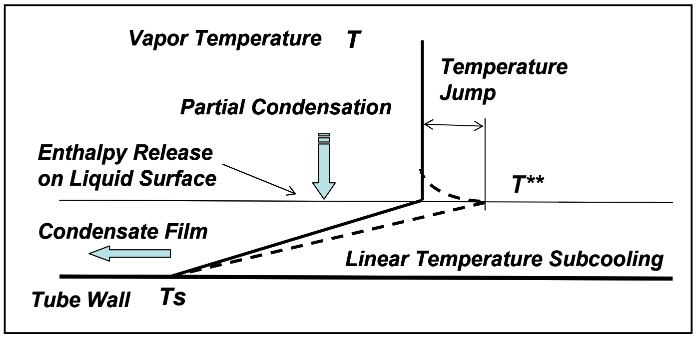

Figure 14 Schematic picture of a temperature jump on the surface of condensate film.

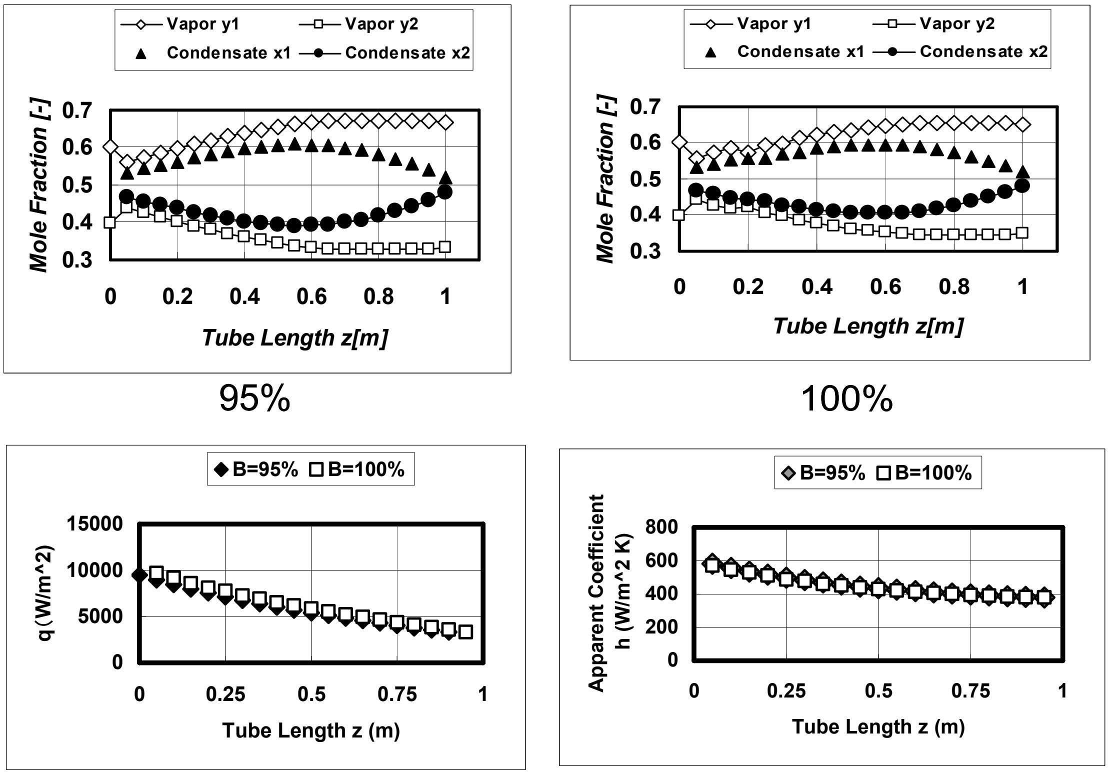

95%

100%

Figure 15 Effect of non-equilibrium on composition trajectory, heat-flux and apparent heat transfer coefficient. $P = 1.5$ atm, $T_F = 110$℃, $Ts = 95$℃, $F = 0.01$ mol/s, $y_{F,1} = 0.600$

Figure 15 shows a comparison between the isothermal equilibrium model (B=100%) and the non-equilibrium model (95%). It seems to be difficult to discern a difference in composition trajectory between these two models. According to the simulation result about local variation of phase equilibrium coefficient, the modification coefficient

$B = 95\%$ corresponds to a temperature jump of the liquid surface of the order of 2 degree Celsius, although depending on specified conditions. Considering the inlet temperature difference $T_F - T_S = 15$ C., this assumed degree of deviation is larger than the conjectured value. Figure 15 indicates that the non-equilibrium model for B=95% estimated the heat-flux to be by 2 % on the average lower than the isothermal equilibrium model (B=100%). This may suggest that the influence of non-equilibrium on the heat transfer rate is not so large for such a large temperature jump in this HIDiC system. It has been found from the same figure that there is no difference in heat transfer coefficient (apparent coefficient) owing to the cancellation between the underestimated temperature difference and the reduced heat-flux.

CONCLUSION

(1) The isothermal equilibrium model proposed in this work can predict various aspects of heat and mass transfer characteristic data useful to design heat transfer tubes for the purpose of HIDiC systems. Only the vapor feed rate is the control parameter which can freely be chosen. The rate of heat transfer is proportional to the vapor feed rate, irrespective of heat transfer condition. As far as the same heat transfer conditions are given, the concentration of less-volatile component depending on the feed vapor temperature and pressure is the second parameter controlling the condensation heat transfer.

(2) A non-equilibrium model was also proposed taking into account a temperature jump on the liquid surface of condensate stream formed due to a large release of enthalpy of phase transition in partial condensation. Even if the temperature jump is estimated large (e.g. of the order of 2 degree Celsius), the total heat transfer rate will not be reduced so largely (e.g. by approximately 2% only). The average heat transfer coefficient remains almost unchanged owing to the cancellation between the underestimated driving force and the reduced heat-flux.

Acknowledgement

This project was financially supported by the New-Energy and Industry Technology Development Organization (NEDO): Global Warming Prevention Technologies Project No. P02020.

REFERENCES

Horiuchi, K., Y. Shibata, K. Yanagimoto, K. Kataoka and M. Nakaiwa, “Computational Energy-Saving Analysis of Multi-Component Petroleum Distillation in a Commercial Scale Heat Integrated Distillation Column,” Proc. 7th World Congress of Chemical Engineering, July. 10-14, Glasgow, CD-ROM (2005)

Kataoka, K., H. Noda, T. Mukaida, M. Kaneda, N. Kuratani, H. Yamaji and M. Nakaiwa, “Non-equilibrium Model of Vapor Condensation in a Heat Transfer Tube for Heat Integrated Distyillation,” Proc. 7th World Congress of Chemical Engineering, July. 10-14, Glasgow, CD-ROM

(2005)

Kjelstrup, S. and D. Bedeaux, “Heat and Mass Transfer across Phase Boundaries: Estimates of Coupling Coefficients,” Proc. 7th World Congress of Chemical Engineering, July. 10-14, Glasgow, CD-ROM (2005)

Kreith, F.,”Principles of Heat Transfer,” 3rd ed., Intext Press (New York), p.527 (1976)

Lueprasitsakul, V., S. Hasebe, I. Hashimoto and T. Takamatsu, “Study of Energy Efficiency of a Wetted-Wall Distillation Column with Internal Heat Integration,” J. Chem. Eng. Japan, 23, 580-587 (1990a)

Lueprasitsakul, V., S. Hasebe, I. Hashimoto and T. Takamatsu, “Analysis of the Characteristics of a Binary Packed Distillation Column with Internal Heat Integration,” J. Chem. Eng. Japan, 23, 686-691 (1990b)

Nakaiwa, M., M. Owa, T. Akiya, S. Kawasaki, V. Lueprasitsakul, K. Yajima and T. Takamatsu, “Design Procedure for a Plate-to-Plate Heat-Integrated Distillation Column,” Kagaku Kogaku Ronbunshu, 12, 535-541 (1986)

Nakaiwa, M., K. Huang, A. Endo, T. Ohmori, T. Akiya and T. Takamatsu, “Internally Heat-Integrated Distillation Columns,” A Review, Trans IChemE, 81, Part A, 162-177. (2003)

Noda, H., N. Kuratani, T. Mukaida, M. Kaneda, K. Kataoka, H. Yamaji and M. Nakaiwa, “Plate Efficiency and Heat Transfer Characteristics in Heat-Integrated Distillation,” Proc. of 10th APCChE Congress, Paper No.017, Oct. 17-21, Kitakyushu, Japan, CD-ROM (2004)

Takamatsu, T., V. Lueprasitsakul and M. Nakaiwa, “Modeling and Design Method for Internal Heat-Integrated Packed Distillation Column,” J. Chem. Eng. Japan, 21, 595-601 (1988)